Effect of Clutter Topology on Multi-Hop Localizer Placement

Muzammil Hussain, Niki Trigoni
Department of Computer Science, University of Oxford
Oxford, United Kingdom
{muzammil.hussain, niki.trigoni}@cs.ox.ac.uk

***Abstract*—Accuracy in range-based localization systems can degrade rapidly in the presence of clutter in the environment. This is due to the incidence of Non-Line-of-Sight (NLOS) distance measurements between the anchors and an unlocalized node. While a large corpus of research work dealt with the scenario where the NLOS distances form a minority of the total distances to anchors, there has been not much research done to handle the situation where a majority or even all distance measurements to anchors are NLOS in nature. In our previous work, we showed that using localizers in a cluttered environment can improve the localization accuracy of a target node even when all the distance measurements are NLOS. Instead of NLOS bias, these techniques suffer residual multi-hop error, which is caused due to the distance overestimate when a multi-hop chain is used instead of the straight-line distance. In this paper, we analyze the effect of clutter topology on the multi-hop error. We use machine learning techniques to estimate the aggregate forms of the multi-hop error for a given clutter topology when only characteristic features of the clutter topology are provided.**

I. Introduction

Localization is a vital service in the area of wireless sensor and robotic networks (WSRNs) since the rationale behind deploying them in the first place is to accomplish tasks based on a spatial dimension in the environment - be it collecting sensor robot measurements or actuation under certain conditions. Motivating applications include exploration/mapping of industrial aqueous tanks with submersible robots and robotic exploration of disaster zones. Range-based localization offers a popular, low-cost method of localization in WSRNs, where an unlocalized robot/node takes distance measurements to a number of anchors, special purpose nodes with known positions, and calculates its position. However, localization accuracy is severely debilitated in the presence of obstacles between the anchors and the unlocalized sensor due to the occurrence of reflected non-line-of-sight (NLOS) distance measurements. The large positive biases of NLOS distances typically result in even larger localization errors.

Current NLOS mitigation techniques [5], [19], [29] require that the number of NLOS distances form the minority of anchors distances, thus not being effective for deployments in severely cluttered environments. Hussain et. al. [15], [16] show that by placing intermediate *localizer* nodes in strategic positions in the clutter, the DV-Distance multi-hop localization technique [23], [22] can offer superior performance even in scenarios where all anchor distances are NLOS in nature. The APDV algorithm proposed in Hussain et al. [16] can be practically deployed on actual robots as it does not require prior clutter topology information nor classification of LOS/NLOS distances. Here, instead of NLOS bias, these techniques suffer multi-hop residual error caused due to the distance overestimate when a multi-hop localizer chain is used instead of the straight-line distance.

However, the efficacy of the above techniques is limited by the clutter topology itself, since certain clutter topologies with large size clutter yield large multi-hop distance errors even when localizer placement is employed. In this paper, we investigate the influence of clutter topology on the localizer placement and multi-hop error when DV-Distance is used. We first look at how different clutter classes affect the distance/localization error as well as the number of required localizers. We then explore aggregate forms (mean, median, maximum) of the multi-hop error for a given clutter topology, using the characteristic features of the clutter topology. Our results can be used to assess if shortest path distance (SPD) based multi-hop localization algorithms, such as DV-Distance and MDS-MAP, can be employed to achieve a desired localization accuracy in a given clutter topology. To summarise, the key contribution of this paper lies in assessing the impact of clutter on the performance of existing multi-hop localisation algorithms.

The remaining paper is organized as follows: in Section (II), we give the background for this work and describe the optimal localizer placement algorithm in more detail; in Section (III) we look at the performance of the OPDV algorithm for different clutter topology classes; in Section (IV), we look at the estimation of aggregate values of multi-hop error using features of the clutter topology; and finally conclude and discuss future work in Section (VI).

II. Background

In this section we will discuss the background for this paper. We start by briefly recollecting the DV-Distance multi-hop localization algorithm. The paper uses the concept of localizers, nodes that assist a given target node to localize better in cluttered environments, proposed in [15], [16]. Localizers are typically mobile nodes that can ideally move in the cluttered environment to assist the target node to localize with better accuracy. An optimal localizer placement algorithm, such as

M. Hussain is presently associated with Samsung Research Institute (SRI) Delhi, Noida, India. Email: muzammil.h@samsung.com

978-3-901882-63-0/2014

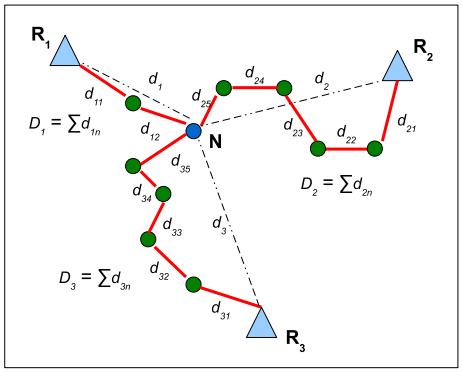

Fig. 1. Node N uses DV-Distance to localize itself. Note that the estimated distances between N and references R_2 and R_3 differ significantly from the true distances.

the Optimal Placement for DV-Distance (OPDV) algorithm, tries to find the optimal positions of these localizers in the cluttered environment to maximize the localization accuracy of the target node. The OPDV algorithm will be used throughout this paper to represent the (lower bound) multi-hop error when DV-Distance is used in cluttered environments.

A. DV-Distance

DV-Distance is a multi-hop localization technique initially devised to localize large networks of wireless sensor nodes [22] with sparse anchor distributions. Anchors typically broadcast position information to their neighboring (unlocalized) nodes. These neighbors record this information, namely anchor positions and distances to anchors. They then broadcast this information in their own vicinities. The nodes that receive these advertisements record their distance to an anchor as the sum of their distance to the advertising node and that node's distance to the anchor, and so on. Thus, in effect the multi-hop distances to the anchors are used instead of the (unavailable) single-hop distances. Fig. (1) shows an example of how node N estimates multi-hop distances to each of the three anchors. One can notice that the node N has significant distance errors for anchors R_2 and R_3 given the zig zag placement of the intermediate nodes.

B. OPDV Algorithm

The **O**ptimal **P**lacement for **DV**-Distance (OPDV) algorithm aims to find the positions of localizers in a cluttered environment such that the multi-hop distances between the anchors and the sensor robot are minimized, thereby minimizing the localization error of the DV-Distance algorithm. The OPDV algorithm makes the following assumptions: the clutter topology is known; the localizers can be placed accurately in desired positions in the cluttered environment; the communication range of the anchors and the localizers follows a simplified disc model; and unlocalized node position is known a priori. Thus, the OPDV algorithm is an oracle-type algorithm, not suitable for actual practical deployment.

The basic version of the OPDV algorithm, which does not impose any constraints on the number of localizers, uses A*

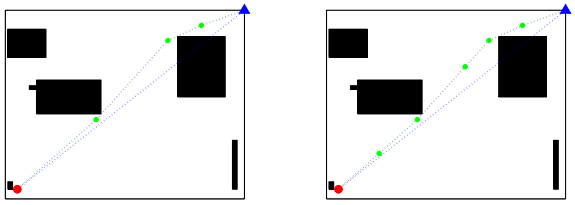

(a) $\mathcal{R}_c$ = 0.25D (b) $\mathcal{R}_c$ = D

Fig. 2. Sample output for the basic version of the OPDV algorithm for different communication ranges. Multi-hop error is expressed in terms of the enclosure diameter D. In both cases, the multi-hop error is 0.0188D.

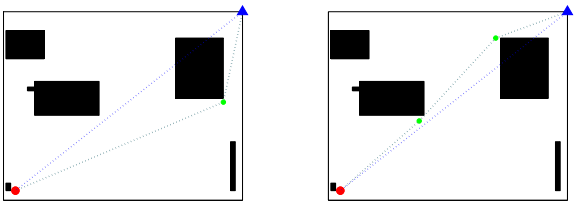

(a) N_{loc}: 1, Multi-hop error: 0.093D (b) N_{loc}: 2, Multi-hop error: 0.0194D

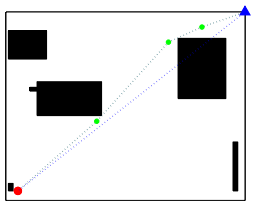

(c) N_{loc}: 4, Multi-hop error: 0.0188D

Fig. 3. Example output of constrained-localizer version of the OPDV algorithm. The multi-hop error is expressed in terms of the diameter of the enclosure D. The communication range of both anchors and localizers is set to D.

graph search [8], [25] to find minimum cost multi-hop paths around the clutter. A* search uses greedy best-first search to find a least-cost path between the source and the destination. The input graph is built using a number of parameters like communication range (anchor and localizer) and grid spacing for candidate localizer positions. In Fig. (2), we see an example of OPDV's output for two values of communication range, 0.25D and D (D is the diameter of the enclosure). Intuitively, the smaller the communication range, the more localizers are needed for the optimal placement.

In a practical deployment scenario, it is vital to be able to work with a limited supply of localizers, N_{loc}. A constrained-localizer version of the OPDV algorithm can be constructed using the Bellman-Ford shortest path algorithm [6] for computing the shortest paths for a given maximal hop-count H. This implementation is based on the property of the Bellman-Ford algorithm that, at its k^{th} iteration, it identifies the optimal path between a given source and each destination among paths of at most k hops. In order to obtain the minimum cost path between the source and all other vertices for a given maximal

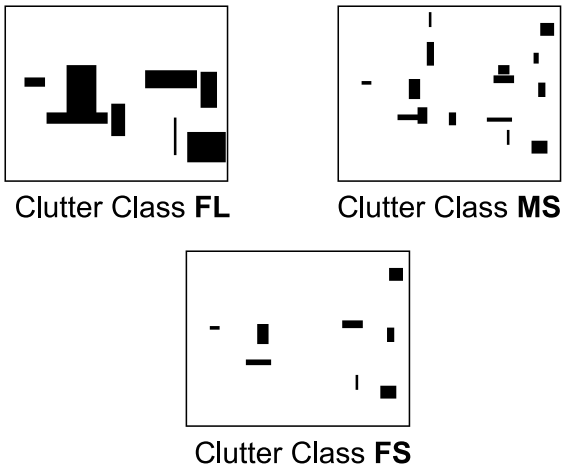

Fig. 4. Samples of the clutter topology classes FL, MS and FS.

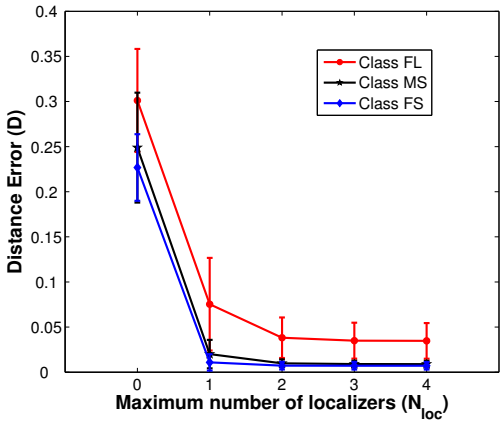

Fig. 6. Influence of clutter topology on distance error of constrained-localizer version of OPDV.

hop-count H, we repeatedly relax all edges of the input graph at most H instead of originally $N-1$ times, where N is the number of vertices in the input graph. Fig. (3) shows an example output of the localizer-constrained OPDV algorithm for a number of localizer constraints $N_{loc}=1$, $N_{loc}=2$ and $N_{loc}=4$. We see that increasing the localizer limit from one to two offers the most improvement in multi-hop error.

The output of OPDV depends on the selection of the grid size. A larger grid size would lead to 'looser' multi-hop paths around the clutter due to the sparser distribution of grid points during the construction of the input graph by the OPDV algorithm. This in turn results in larger overestimate errors in the shortest length multi-hop paths found by OPDV.

III. Effect of clutter topology on multi-hop distance error

In this section we evaluate the performance of the OPDV algorithm for different classes of clutter topology. We also compare OPDV to other single-hop localization techniques to illustrate the advantages of using localizer placements.

First, we define three clutter topology classes, namely the FL (few large clutter objects), MS (many small clutter objects) and FS (few small clutter objects). The clutter classes signify the variations in sizes of the obstacles and the amount of clutter in the environment. Samples for each class is shown in Fig. (4) .

Next, we evaluate the effect of clutter topology on OPDV distance error, while at the same time comparing OPDV's performance to that of two single-hop localization techniques, linear least squares estimation (LLSE) and upper-bound least squares estimation (UBLSE) [29]. For evaluation, 30 clutter topologies are randomly chosen for each class, and for each clutter topology, 100 random positions for the unlocalized node are generated. For each such position, we first evaluate whether it has LOS or NLOS distances with each of the four anchors. LOS distance error is set to 0 while NLOS distance error is obtained through ray tracing. In case of OPDV, the distance error, if any, is due to the overestimating nature of the multi-hop paths. The results are shown in Fig. (5). Both, the NLOS error and the multi-hop error in OPDV-based DV-Distance, decrease as the clutter size decreases in size. However the NLOS error is many times greater than the multi-hop error, being 8.5 times in case of the FL clutter class, to as much as 39 times in case of the FS clutter class. Since distance error is a major source for localization error, one can see the immense benefits of using OPDV-based multi-hop localization in such scenarios. UBLSE is known to perform well in situations where the NLOS distances form a minority of all distances to anchors. Hence, on average, it performs much better than LLSE. We can conclude that OPDV offers the most benefit when compared to single-hop localization techniques for lightly cluttered environments, though even with the FL clutter topology class, OPDV performs better than UBLSE by a factor of 2x.

Next, we investigate the influence of clutter topology on the distance error of the constrained-localizer version of OPDV. Again, we consider 30 clutter topology samples from each clutter class with 30 random positions for the unlocalized node and anchor (anchor positions being confined to the enclosure boundary). The constrained-localizer version of OPDV is applied to each pair of sensor robot and anchor position, with N_{loc} being varied from 0 to 4. The results are shown in Fig. (6). We find that clutter class FL shows the error with the largest magnitude and variance, while clutter classes MS and FS yielding smaller distance errors. We find that the improvement in distance errors when a single localizer is added varies substantially between the various clutter classes, with clutter class FL yielding a gain of 75%, clutter class MS yields a gain of 91% and clutter class FS yielding a gain of 98%. We also find that two localizers are sufficient to get the maximum benefit in terms of error reduction for all clutter classes. This observations suggests that a small practical number of localizers can indeed be allocated to obtain significant benefits in terms of localization accuracy.

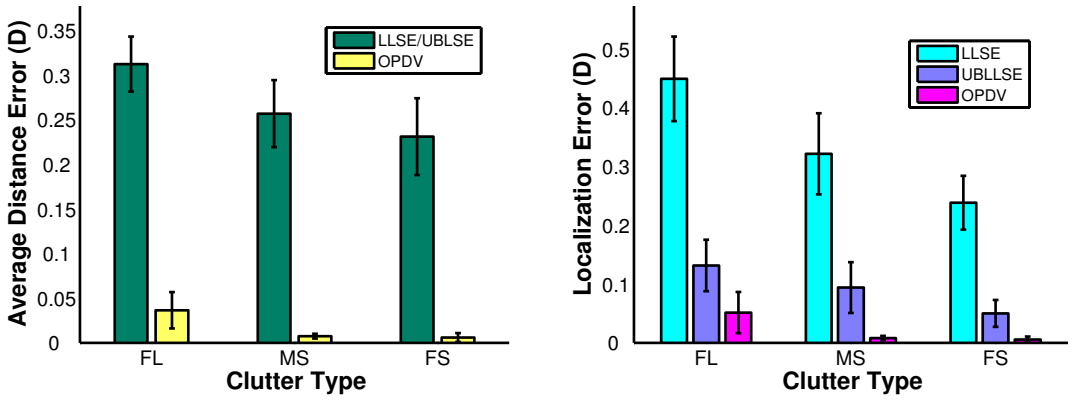

(a) Average Distance Error (b) Localization Error

Fig. 5. Comparison of the performance of OPDV with single-hop localization techniques for different classes of clutter topologies.

We can conclude that the size of the clutter has a much more significant impact on the OPDV distance error than the number of clutter objects in the environment.

IV. Estimation of OPDV multi-hop error from clutter topology features

In the previous section, we looked at the effect of various clutter topology classes on the distance error of single-hop and multi-hop distance measurement modes. We saw that, intuitively, clutter topologies with larger size clutter give higher localization errors. In this section, we will look at estimating the distance error itself, particularly the multi-hop overestimate error, for a given clutter topology. Previous work [14] showed that it is possible to estimate single-hop distance error, specifically the NLOS incidence probability and bias distribution, from characteristic features of a given clutter topology. In this section, we extend that work to the estimation of multi-hop overestimate error when a chain of localizers form multi-hop distances between the anchors and the unlocalized node. We focus on the multi-hop error when OPDV is used since it represents the lower bound of the overestimate error in the multi-hop distances when localizers are used.

A. Clutter Topology Features

In this section we will summarize various characteristic features related to a clutter topology, previously introduced in Hussain et al. [14]. These features are various forms of representing the spacing between the clutter objects.

Clutter Area Fraction: The ratio of the clutter area to the total area, ca, is an important indicator of the level of clutter in the environment.

Clutter Spacing Distribution: The space in midst of the obstacles and bounding enclosure plays a vital role in determining the NLOS distance biases. We define two types of clutter spacing distributions: *linear* ($\mathcal{CD}_l$) spacing distribution is obtained by measuring the space from a random position in the clutter topology (outside any obstacle) in a random direction till it strikes an obstacle or the enclosure walls in its path; and *radial* ($\mathcal{CD}_r$) spacing distribution is obtained by measuring the maximal radius of the circle that can be drawn centered at a (random) point such that it does not intersect an obstacle or the enclosure walls. Examples of the construction of $\mathcal{CD}_l$ and $\mathcal{CD}_r$ are provided in Figs. (7) and (8) respectively.

Occupancy Grid: The occupancy grid of the clutter topology

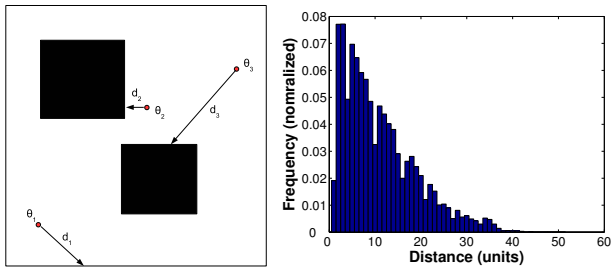

(a) Samples for $\mathcal{CD}_l$ (b) $\mathcal{CD}_l$ obtained with 1000 samples

Fig. 7. Derivation of linear clutter spacing distribution, $\mathcal{CD}_l$. Here, three random points are chosen along with three random direction θ_1, θ_2 and θ_3, that give the corresponding spacing distances d_1, d_2 and d_3. In practice, one can build these distributions with 500 or 1000 samples points.

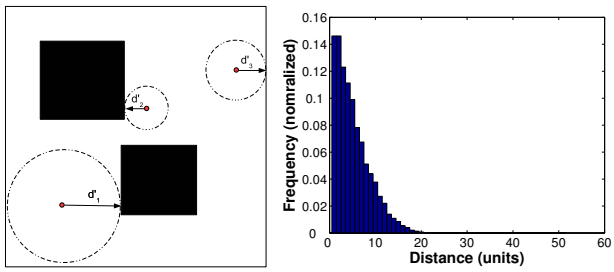

(a) Samples for $\mathcal{CD}_r$ (b) $\mathcal{CD}_r$ obtained with 1000 samples

Fig. 8. Derivation of radial clutter spacing distribution, $\mathcal{CD}_r$. Here, three random points are chosen along with three random direction θ_1, θ_2 and θ_3, that give the corresponding spacing distances d'_1, d'_2 and d'_3 that represent the radii of the smallest circles that can be fitted before touching, in the *first* instance, a clutter piece or the enclosure wall. In practice, one can build these distributions with 500 or 1000 samples points.

is a literal representation of the actual map of the clutter topology scaled by a factor s. In other words, if occ_1 represents the matrix representation of the clutter topology, with 1s denoting the enclosure boundaries and clutter and 0s denoting free space, occ_S is the corresponding matrix with dimensions scaled by a factor of S, where $S = \frac{norm([X_L^O Y_L^O])}{norm([X_L Y_L])}$ and (X_L^O, Y_L^O) are the original dimensions of the clutter map image and (X_L, Y_L) are the dimensions of the scaled image. For example, if occ_1 is a 100x100 matrix, then $occ_{12.5}$ will be represented by a 8x8 matrix and $occ_{3.125}$ by a 32x32 matrix. We select a bi-linear interpolation scheme for matrix compression.

Fourier Transformation: The Fourier transform is a popular representation in the image processing research community [9], [27], [20]. It highlights the dominant spatial frequencies as well as the dominant orientations of the structures contained in the image. The Fourier transformation of an image provides its representation in the frequency domain. A two dimensional Fourier transformation (ft_S) of the occupancy grid occ_S, where S is the scale factor of the occupancy grid, is used to characterize the spacing and structure of the clutter. We use the magnitude of the 2D Fourier transform as the feature in our analysis.

GIST Characterization: The GIST [24] ($\mathcal{G}$) characterization of an image, widely used in the area of image classification, defines a set of 'perceptual' dimensions that represent the dominant spatial structure of the image. The technique can be used to capture low level details of the image, for example in our case, the spacing and shapes of the clutter topology, while abstracting away the high-dimensional detail.

B. Experimental Setup

In this section, we will describe the setup for generating the experimental data. We aim to evaluate the multi-hop distance error when one or more localizers are used between an anchor and an unlocalized node. We use the basic version of the OPDV algorithm, which does not impose any constraint on the number of localizers. The reason for this is that here we want to understand the multi-hop distance error with respect to only the clutter topology. By introducing a localizer limit (N_{loc}) factor, we will introduce another external factor for the multi-hop distance error. For the same reason, we set the communication range of both anchors and localizers to the maximal value of D, the diameter of the cluttered environment. The position of the anchor is randomly chosen along the boundary of the enclosure, while a random position in the enclosure, not occupied by clutter, is chosen for the unlocalized node. For each clutter topology sample, we calculated the OPDV multi-hop paths for $N_o(= 1000)$ pairs of anchor and unlocalized node positions. The multi-hop error is calculated as the overestimate in the cumulative multi-hop distance when compared to the true distance.

Clutter Topology Generation: We build complex clutter topologies by sequentially overlaying simple rectilinear structures over each other. We use a 2D rectangular enclosure area with dimensions L_x and L_y. We then generate ncl boxes with random start points (x_i, y_i) and dimensions lx and ly, where

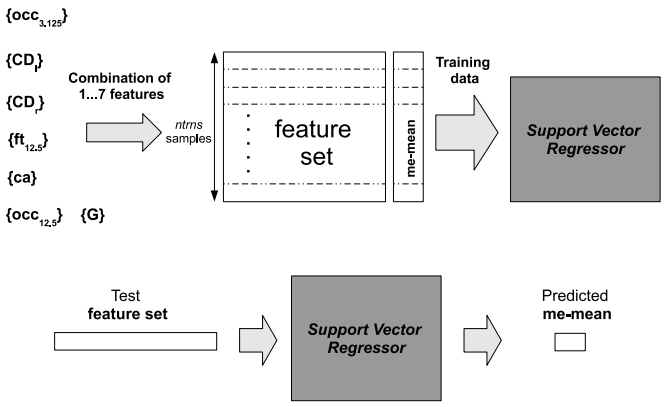

Fig. 9. Estimation of mean OPDV multi-hop error (*me-mean*) using Support Vector Regressor (SVR). A similar procedure is used for estimating median multi-hop error (*me-median*) and maximum multi-hop error (*me-max*).

$lx = \mathcal{U}(x_i, x_i + \frac{L_x}{dimfac})$ and $ly = \mathcal{U}(y_i, y_i + \frac{L_y}{dimfac})$. The values of ncl and $dimfac$ are determined by the clutter class. For each sample, we first randomly choose a clutter topology class from the three clutter classes FL (few large-size clutter), MS (many small-size clutter) and FS (few small-size clutter). In case of clutter class FS, we set ncl as a randomly chosen natural number between [1, 8] and $dimfac$ = 3. In case of clutter class MS, ncl is randomly chosen between [1, 20] and $dimfac$ = 8. Finally, in case of clutter class FS, ncl is chosen between [1, 8] and $dimfac$ is set to 8.

Support Vector Regression: We use a Support Vector Regressor (SVR) for predicting the aggregate multi-hop error, given characteristic features of a clutter topology. An ϵ-SVR [7], [26] solves the following optimization problem:

$$\text{minimize } \frac{1}{2}\|w\|^2 + C\sum_{i=1}^{l}(\zeta_i + \zeta_i^*) \qquad (1)$$

$$\text{subject to } \begin{cases} y_i - < w, x_i > -b & \leq \epsilon + \zeta_i \\ < w, x_i > +b - y_i & \leq \epsilon + \zeta_i^* \\ \zeta_i, \zeta_i^* & \geq 0 \end{cases}$$

where ζ_i and ζ_i^* are slack variables and ϵ is the precision. The unknown parameters, w and b, are determined based on the training set $\{x_k, y_k\}_{k=1}^N$, where $x_k \in \mathbb{R}^n$ is the input and $y_k \in \mathbb{R}$ the respective output. In our case, the input x_i represents the feature set $\mathcal{F}^n$ of the i^{th} clutter topology sample, where n denotes the number of features we are considering at a time. The output is an aggregate form of the multi-hop error for the clutter topology. We found that non-linear ϵ-SVR together with the Radial Basis (RBF) kernel gives the best results during our analysis, when compared to linear, polynomial and sigmoid kernels.

C. Results

In this section, we will look at the estimation of the OPDV multi-hop error for an arbitrary clutter topology when we are only given features characterizing the clutter topology. We use

a combination of various features of the clutter topology to predict mean multi-hop error (*me-mean*), median multi-hop error (*me-median*) and maximum multi-hop error (*me-max*). Fig. (9) shows the schematic diagram for the entire process of training and predicting *me-mean* with the SVR. Identical processes are used for estimating *me-median* and *me-max*.

For a given test clutter topology, we represent the estimation error for multi-hop error mean as $err_{me-mean}$, the estimation error for multi-hop error median as $err_{me-median}$ and the estimation error for the multi-hop error maximum as err_{me-max}. The error is taken as the absolute difference between the true and estimated values. The performance of the individual features for each of the aggregate values of multi-hop error is shown in Fig. (10). Similarly, the best performances of using 2, 3 and 4 feature combinations for *me-mean*, *me-median* and *me-max* are presented in Tables (I), (II) and (III) respectively.

We see that features $occ_{3.125}$, $occ_{12.5}$ and $ft_{3.125}$ perform the best among all other features. $ft_{3.125}$ performs the best in case of estimating *me-mean* and *me-median*, while $occ_{12.5}$ offers the highest estimation accuracy for *me-max*. We see that using combinations of two or more features does not lead to any significant improvement in estimation accuracy. We also see that the standard deviations for all the estimations are larger than the means, indicating that the SVR estimator is not able to perform well for a small minority of test samples, which give large estimation errors. Nevertheless, these results show that employing clutter topology information delivers much better performance than the baseline, which simply represents the average of all training data, in the estimation of the multi-hop error. We are able to predict the mean, median and maximum OPDV error with an average error of only 0.72, 0.41 and 8.69 units respectively, for an enclosure area of 10,000 square units.

We note that the spacing distributions, CD_l and CD_r do not perform as well as the other features. The reason could be that the multi-hop path between the anchor and the unlocalized node in the clutter is hardly affected by the spacing between the clutter objects. Instead they depend on the positions of the clutter with respect to the positions of the two nodes. In case of estimation of NLOS incidence probability [14], the spacing between the clutter indirectly determines that probability of an NLOS distance between two random points in the given cluttered environment. Similarly, the spacing between the clutter objects has a strong influence on the length of the reflected signal that determines the NLOS bias. Thus, we see that multi-hop error is mainly determined by the relative positions of the clutter objects with respect to the enclosure, represented by the features $occ_{12.5}$, $occ_{3.125}$ and $ft_{3.125}$.

V. Related Work

Previous literature have attempted to characterize NLOS bias for NLOS mitigation techniques [31], [10], [21], [12], [13], [17]. These characterizations range from variance of NLOS distances [31] to multipath channel statistics (in case of Ultrawide Band (UWB) signals), namely the kurtosis and the mean excess delay of the multipath channel. Similarly, Marano et al. [21] employ various characteristics of the impulse response of the received UWB signal. Position Error Bound (PEB) [18] uses empirically derived NLOS bias distributions for its NLOS mitigation scheme. A number of papers [11], [12] also assume exponential NLOS error distributions, while [28], [17] assume a uniform distribution within a predefined range. Other works have furthermore assumed that NLOS bias follows a Gaussian distribution [4] as well as a non-parametric Gaussian kernel density function [13].

The effect of clutter topology on the NLOS bias has also been studied in a number of papers [30], [2], [1]. Wang et al. [30] deduce that NLOS error is strongly dependent on the clutter geometry and is frequency-dependent for severe clutter. Alsindi et al. [2] conclude that the NLOS bias follows a log-normal distribution with large bias forming the long tail, when there is an obstruction between the two ranging nodes. Furthermore, the authors show that the parameters of this lognormal distribution is dependent on the clutter environment and system bandwidth [3], [1].

However, our work is the first to study the effect of clutter topology on multi-hop overestimate error, when multi-hop node chains (as compared to direct NLOS links) between the anchors and an unlocalized node are employed. Previous work [15], [16] has shown that multi-hop localization offers a better alternative in severely cluttered settings.

VI. Conclusion and Future Work

In this paper, we looked at the problem of optimal placement of intermediate localizer nodes to enhance the localization accuracy in cluttered NLOS-prone environments, and the effect of clutter topology on the residual multi-hop error. We saw that the size of the clutter affects the multi-hop error of optimal localizer placements more than the number of clutter objects present in the environment. In case of estimation of the aggregate values of the multi-hop error from the features of a given clutter topology, we see that features that require complete clutter topology information such as occupancy grids perform better than clutter spacing distributions, given the minor influence of spacing between clutter objects on the overestimate error of the multi-hop paths. The estimation of aggregate of multi-hop error is useful for evaluating whether a given distance error (and subsequently localization accuracy) can be obtained in a given clutter topology when shortest-path distance based multi-hop algorithms, such as DV-Distance and MDS-MAP, are used. For future work, we plan to extend this work to the optimal placement of a fixed number of localizers that minimize aggregate localization error over an entire deployment area.

VII. Acknowledgments

This work is supported by EPSRC grants AASN4IP EP/F064209/1 and HARPS EP/L00416X/1. We would like to acknowledge Yusuf Aytar, Oxford University, for his useful insights for the estimation of multi-hop error from clutter topology information.

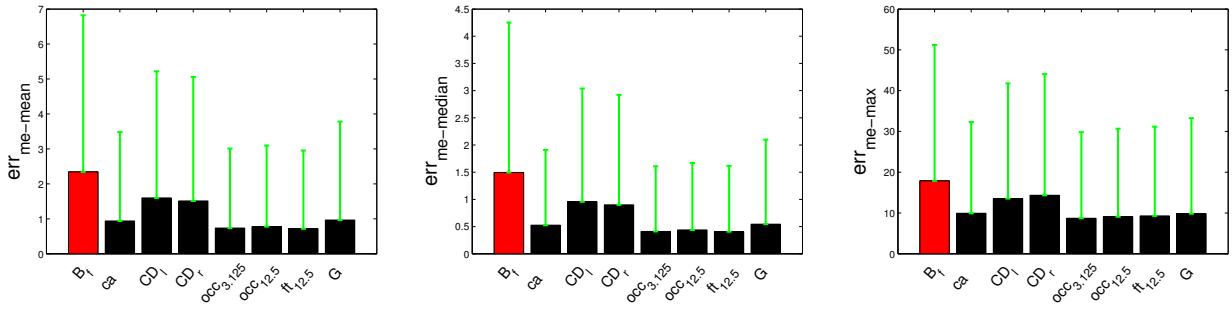

(a) Estimation accuracy of *me-mean*. (b) Estimation accuracy of *me-median*. (c) Estimation accuracy of *me-max*.

Fig. 10. SVR based estimation of *me-mean*, *me-median* and *me-max* with individual features of clutter topology.

Estimation Technique using SVR	$err_{me-mean}$ (mean)	$err_{me-mean}$ (std)
$\mathcal{B}_{me-mean}$	2.3425	2.1367
$\mathcal{F}^1_{me-mean} = \{ft_{3.125}\}$	0.7139	1.5251
$\mathcal{F}^2_{me-mean} = \{occ_{3.125}, ft_{3.125}\}$	0.7166	1.5243
$\mathcal{F}^3_{me-mean} = \{occ_{12.5}, occ_{3.125}, ft_{3.125}\}$	0.7167	1.5230
$\mathcal{F}^4_{me-mean} = \{ca, occ_{12.5}, occ_{3.125}, ft_{3.125}\}$	0.7164	1.5227

TABLE I

ESTIMATION OF *me-mean* WITH COMBINATION OF CLUTTER TOPOLOGY FEATURES. HERE, THE SET $\mathcal{F}^i_{me-mean}$ DENOTES THE SET OF i FEATURES WHICH ACHIEVE THE MINIMUM $err_{me-mean}$.

Estimation Technique using SVR	$err_{me-median}$ (mean)	$err_{me-median}$ (std)
$\mathcal{B}_{me-median}$	1.4946	1.2637
$\mathcal{F}^1_{me-median} = \{ft_{3.125}\}$	0.4062	0.8031
$\mathcal{F}^2_{me-median} = \{occ_{3.125}, ft_{3.125}\}$	0.4019	0.7718
$\mathcal{F}^3_{me-median} = \{occ_{12.5}, occ_{3.125}, ft_{3.125}\}$	0.4020	0.7711
$\mathcal{F}^4_{me-median} = \{ca, occ_{12.5}, occ_{3.125}, ft_{3.125}\}$	0.4018	0.7708

TABLE II

ESTIMATION OF *me-median* WITH COMBINATION OF CLUTTER TOPOLOGY FEATURES. HERE, THE SET $\mathcal{F}^i_{me-median}$ DENOTES THE SET OF i FEATURES WHICH ACHIEVE THE MINIMUM $err_{me-median}$.

Feature set	err_{me-max} (mean)	err_{me-max} (std)
$\mathcal{B}_{me-max}$	17.8846	15.4092
$\mathcal{F}^1_{me-max} = \{occ_{12.5}\}$	8.7026	12.4167
$\mathcal{F}^2_{me-max} = \{occ_{12.5}, ca\}$	8.6956	12.4052
$\mathcal{F}^3_{me-max} = \{occ_{12.5}, occ_{3.125}, occ_{3.125}\}$	8.8393	12.4456
$\mathcal{F}^4_{me-max} = \{ca, occ_{12.5}, occ_{3.125}, ft_{3.125}\}$	8.8614	12.7020

TABLE III

ESTIMATION OF *me-max* WITH COMBINATION OF CLUTTER TOPOLOGY FEATURES. HERE, THE SET $\mathcal{F}^i_{me-max}$ DENOTES THE SET OF i FEATURES WHICH ACHIEVE THE MINIMUM err_{me-max}.

REFERENCES

[1] B. Alavi and K. Pahlavan. Modeling of the distance error for indoor geolocation. In *Wireless Communications and Networking, 2003. WCNC 2003. 2003 IEEE*, volume 1, pages 668–672. IEEE, 2003.

[2] N. Alsindi, B. Alavi, and K. Pahlavan. Spatial characteristics of uwb toa-based ranging in indoor multipath environments. In *Personal, Indoor and Mobile Radio Communications, 2007. PIMRC 2007. IEEE 18th International Symposium on*, pages 1–6. IEEE, 2007.

[3] N. Alsindi, B. Alavi, and K. Pahlavan. Measurement and modeling of ultrawideband toa-based ranging in indoor multipath environments. *Vehicular Technology, IEEE Transactions on*, 58(3):1046–1058, 2009.

[4] J. Borras, P. Hatrack, and N. Mandayam. Decision theoretic framework for nlos identification. In *Vehicular Technology Conference, 1998. VTC 98. 48th IEEE*, volume 2, pages 1583–1587. IEEE, 1998.

[5] P. Chen. A non-line-of-sight error mitigation algorithm in location-estimation. In *1999 IEEE Wireless Communications and Networking Conference, 1999. WCNC*, pages 316–320, 1999.

[6] T. Cormen. *Introduction to algorithms*. The MIT press, 2001.

[7] C. Cortes and V. Vapnik. Support-vector networks. *Machine learning*, 20(3):273–297, 1995.

[8] R. Dechter and J. Pearl. Generalized best-first search strategies and the optimality of a*. *Journal of the ACM (JACM)*, 32(3):505–536, 1985.

[9] R. d'Entremont. Performance of the discrete fourier transform satellite imagery classification technique. Technical report, DTIC Document, 1980.

[10] S. Gezici, H. Kobayashi, and H. Poor. Nonparametric nonline-of-sight identification. In *Vehicular Technology Conference, 2003. VTC 2003-Fall. 2003 IEEE 58th*, volume 4, pages 2544–2548. IEEE, 2003.

[11] S. Gezici and Z. Sahinoglu. Uwb geolocation techniques for ieee 802.15. 4a personal area networks. *Mitsubishi Electric Research Laboratory Technical Report TR-2004-110*, 2004.

[12] I. Guvenc, C. Chong, and F. Watanabe. Nlos identification and

mitigation for uwb localization systems. In *Wireless Communications and Networking Conference, 2007. WCNC 2007. IEEE*, pages 1571–1576. IEEE, 2007.

[13] J. Huang and Q. Wan. The crlb for wsns location estimation in nlos environments. In *Communications, Circuits and Systems (ICCCAS), 2010 International Conference on*, pages 83–86. IEEE, 2010.

[14] M. Hussain, Y. Aytar, A. Markham, and N. Trigoni. Characterization of non-line-of-sight (nlos) bias via analysis of clutter topology. In *IEEE/ION PLANS*, 2012.

[15] M. Hussain and N. Trigoni. Distributed localization in cluttered underwater environments. In *Proceedings of the Fifth ACM International Workshop on UnderWater Networks*, page 8. ACM, 2010.

[16] M. Hussain and N. Trigoni. Adaptive node placement for improving localization accuracy in clutter-prone environments. In *IEEE Wireless Communication and Networking Conference (WCNC)*, 2013.

[17] T. Jia and R. Buehrer. Collaborative position location with nlos mitigation. In *Personal, Indoor and Mobile Radio Communications Workshops (PIMRC Workshops), 2010 IEEE 21st International Symposium on*, pages 267–271. IEEE, 2010.

[18] D. Jourdan, D. Dardari, and M. Win. Position error bound for uwb localization in dense cluttered environments. *Aerospace and Electronic Systems, IEEE Transactions on*, 44(2):613–628, 2008.

[19] H. Kung, C. Lin, T. Lin, and D. Vlah. Localization with snap-inducing shaped residuals (sisr): Coping with errors in measurement. In *MOBICOM*, pages 333–344. ACM, 2009.

[20] I. Kunttu, L. Lepisto, J. Rauhamaa, and A. Visa. Multiscale fourier descriptor for shape classification. In *Image Analysis and Processing, 2003. Proceedings. 12th International Conference on*, pages 536–541. IEEE, 2003.

[21] S. Marano, W. Gifford, H. Wymeersch, and M. Win. Nlos identification and mitigation for localization based on uwb experimental data. *Selected Areas in Communications, IEEE Journal on*, 28(7):1026–1035, 2010.

[22] D. Niculescu and B. Nath. Ad hoc positioning system (aps). In *IN GLOBECOM*, pages 2926–2931, 2001.

[23] D. Niculescu and B. Nath. DV based positioning in ad hoc networks. *Telecommunication Systems*, 22(1):267–280, 2003.

[24] A. Oliva and A. Torralba. Modeling the shape of the scene: A holistic representation of the spatial envelope. *International Journal of Computer Vision*, 42(3):145–175, 2001.

[25] S. Russell, P. Norvig, J. Canny, J. Malik, and D. Edwards. *Artificial intelligence: a modern approach*, volume 2. Prentice hall Englewood Cliffs, NJ, 1995.

[26] A. Smola and B. Schölkopf. A tutorial on support vector regression. *Statistics and computing*, 14(3):199–222, 2004.

[27] X. Tang and W. Stewart. Optical and sonar image classification: wavelet packet transform vs fourier transform. *Computer vision and image understanding*, 79(1):25–46, 2000.

[28] S. Venkatesh and R. Buehrer. A linear programming approach to nlos error mitigation in sensor networks. In *Proceedings of the 5th international conference on Information processing in sensor networks*, pages 301–308. ACM, 2006.

[29] C. Wang and L. Xiao. Sensor localization in concave environments. *TOSN*, 4(1):1–31, 2008.

[30] W. Wang, t. Jost, and U. Fiebeg. Characteristics of the nlos bias for an outdoor-to-indoor scenario at 2.45 ghz and 52 ghz. In *IEEE Antannae and Wireless Propagation Letters*, volume 10. IEEE, 2011.

[31] M. Wylie and J. Holtzman. The non-line of sight problem in mobile location estimation. In *5th IEEE International Conference on Universal Personal Communications*, volume 2, pages 827–831, 1996.